

# Swept-wavelength source for optical coherence tomography in the 1 $\mu\text{m}$ range

F. D. Nielsen<sup>1</sup>, L. Thrane<sup>1</sup>, J. Black<sup>2</sup>, K. Hsu<sup>3</sup>, A. Bjarklev<sup>4</sup> and P. E. Andersen<sup>1</sup>

<sup>1</sup>Risoe National Laboratory, Frederiksborgvej 399, DK-4000 Roskilde

<sup>2</sup>Advanced Development Group, Reliant Technologies, 260 Sheridan Avenue, Suite 300, Palo Alto, CA 94306 USA,

<sup>3</sup>Micron Optics Inc., 1852 Century Place NE, Atlanta, GA 30345 USA, E-mail: khsu@micronoptics.com

<sup>4</sup>COM, The Technical University of Denmark, Build 345V, DK-2800 Kgs. Lyngby, Denmark,

Email: [frederik.d.nielsen@risoe.dk](mailto:frederik.d.nielsen@risoe.dk)

## ABSTRACT

Two swept wavelength light sources based on Ytterbium doped fibre amplifiers are demonstrated. The filtered output from a superfluorescent source is scanned over 20 nm, and used for tomography with an axial resolution of <40  $\mu\text{m}$ . Dynamic properties of a swept wavelength YDFA based ring laser is investigated. This is the first reported results with dynamically swept sources centered in the 1  $\mu\text{m}$  wavelength range, which is expected to be important for future development of optical coherence tomography systems for retinal imaging.

## INTRODUCTION

For optical coherence tomography (OCT) applications there has recently been an interest in Fourier domain OCT (FD-OCT) systems, because FD-OCT systems promise improved signal-to-noise-ratio (SNR) compared to time domain OCT [1]. There are currently two general principles that can be used for FD-OCT; spectral OCT and swept-source OCT. In a swept-source FD-OCT system, the optical frequency of the light source is swept during an A-scan. The detector signal from a reflection site varies harmonically as a function of the optical frequency of the light source. The frequency of the harmonic signal is linearly related to the  $z$ -position of the reflection site. Hence, frequency analysis of the detector signal, gives  $z$ -resolved reflection information from the sample. The axial resolution of FD-OCT systems is inversely proportional to the scanned bandwidth and given by [2]:

$$\Delta z = \frac{\lambda_0^2}{2n\Delta\lambda},$$

where  $n$  is the refractive index of the sample,  $\lambda_0$  the centre wavelength of the light source and  $\Delta\lambda$  the swept wavelength interval and it has been assumed that the light source has a rectangular shaped spectrum. Selection of the centre wavelength for the light source must be done in accordance with the application, where scattering and absorption losses should be considered. One successful application of OCT today is within the field of ophthalmology, where imaging of deeper lying retinal features is accomplished as a part of everyday clinical practice. For this application, it has been shown that a centre wavelengths in the 1-1.1  $\mu\text{m}$  range is well suited [3]. The highly scattering and absorbing *retinal pigment epithelium* reduces the penetration depth for wavelengths 800 nm range commonly used today in retinal scanning OCT systems, while going to longer wavelengths is limited by water absorption in relative long path through the *vitreous humor*. However, a through investigation by Unterhuber et. al. showed, in the 1  $\mu\text{m}$  range, a suitable compromise between water absorption, scattering loss in the retina and the maximum permissible exposure, according to the ANSI standard, is found in the 1  $\mu\text{m}$  [4]. Furthermore, a significantly better penetration depth was demonstrated using a superfluorescent light source, based on an Ytterbium doped fibre amplifier (YDFA), compared to that obtained with a Ti:sapphire laser [4].

The combination of FD-OCT and operation in the 1  $\mu\text{m}$  range is therefore of great practical interest. YDFAs offer a broad amplification bandwidth in 1  $\mu\text{m}$  range and commercially available, making them attractive for this application but have yet to demonstrated in Fourier domain configurations.

Various methods have been demonstrated in making tunable sources, such as for example Littrow/Littman type cavities, and temperature tuned semiconductor lasers. However, the single mode operation offered by such designs can be sacrificed in the quest for larger scanning speeds, since the required coherence length needed for FD-OCT is generally in the order of 1-2 cm, depending on the requirements for probing depth and sensitivity. Multi longitudinal mode ring cavity designs have therefore been successfully been applied, offering large bandwidths and fast scanning speeds [5].

In this presentation two YDFA based light sources is investigated; a swept wavelength laser source and a source based on swept filtering of a superfluorescent output from an YDFA. Tomography is performed with the superfluorescent source and a resolution of 35  $\mu\text{m}$  has been achieved.

## YDFA BASED SWEEPED WAVELENGTH RING LASER

Linear cavity designs based YDFAs can suffer from a temporal unstable output power, due to processes such as Brillouin scattering [6]. Tunable cavities tend to have high losses due to the frequency selective element, and high gains are therefore necessary. Especially such high loss cavities exhibit severe temporal instability ranging from regular self-pulsing to completely chaotic domains [6]. Unidirectional ring cavity designs can avoid such instabilities, and provide stable operation over a wide wavelength range. Based on an YDFA, Auerbach et. al. was with such a ring cavity, able to obtain tuning range of 92 nm with output powers up to 10 W [7]. But, in this case tuning of the wavelength was done in steps, not dynamically, as required for FD-OCT.

A unidirectional YDFA based ring laser with a tunable filter was therefore constructed to investigate the properties, whilst scanning the wavelength dynamically. The purpose of the experiment was to evaluate, how output power relates to the scanning speed, and to investigate if it was possible to control the polarization state under dynamic wavelength scanning conditions.

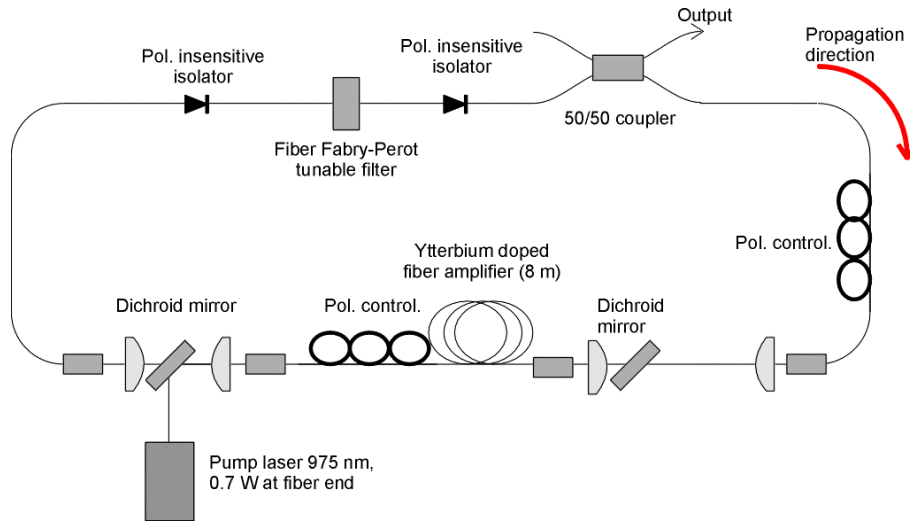


**Figure 1: Swept wavelength ring laser setup**

The experimental setup is shown in Figure 1. The YDFA was a flower shaped double clad structure, and was pump in the opposite direction to the signal path through the amplifier. A broad area laser was used as pump, and was temperature tuned to the peak absorption wavelength of the YDFA at 975 nm. As frequency selective element, a fiber Fabry Perot tunable filter was used (Micron Optics, Inc.). The filter had a free spectral range of 47 nm and a finesse of 1500. Being a sealed fiber coupled device, it requires no user alignment and offers easy electrical control of the center wavelength. Polarization insensitive fiber isolators were placed on both sides of the filter to avoid reflections from the Fabry-Perot cavity back into the amplifier. Since the dichroic filters, used for pump and signal separation, were sensitive to the polarization of the signal wavelength, polarization controllers were positioned prior to these components in the signal path. The total roundtrip loss in the ring was 16 dB due to coupling loss and insertion loss of the various components in the ring.

The maximum output power from the laser was chosen to be 1 mW, in order to avoid damaging the high finesse Fabry-Perot filter. Positioning the output coupler in the signal path prior to filter section would increase the output power by 5 dB, since insertion loss from the filter and one of the isolators could be avoided.

While keeping the pump power fixed, the output power at the peak wavelength was measured as a function of the scanning speed. A linear relation between scanning frequency and output power was found, as shown in Figure 2.

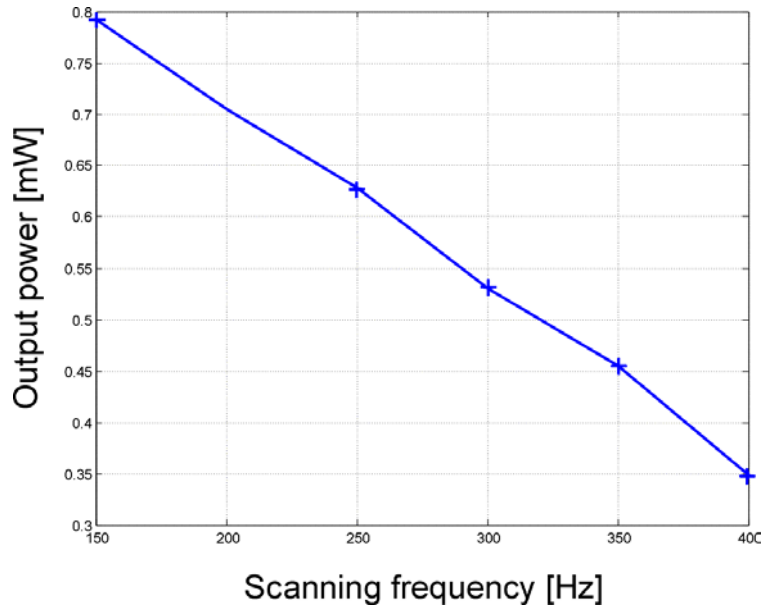


**Figure 2: Output power vs. scanning speed**

The corresponding output spectrum is shown in Figure 3, with scanned bandwidth of 4 nm. The wavelength scale in Figure 3 has been indirectly derived through a filter drive voltage versus center transmission wavelength relation determined experimentally with an OSA and a superfluorescent source.

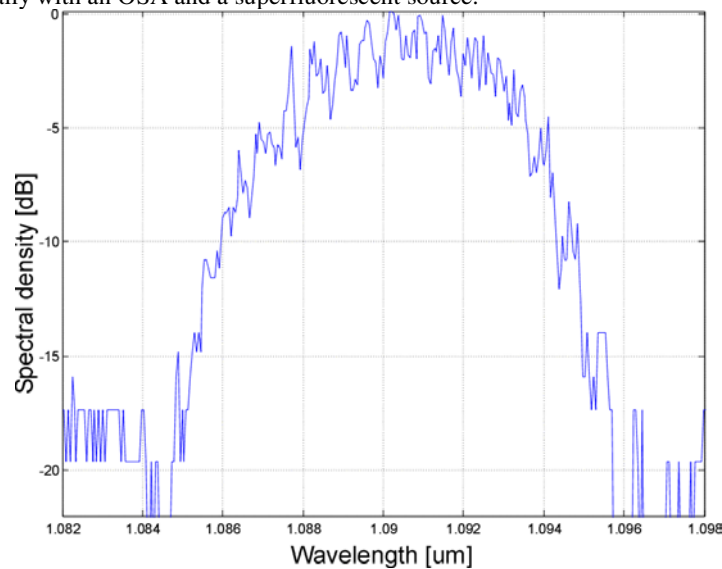


**Figure 3: Output spectrum from the wavelength swept ring laser**

As the dichroic signal/pump combiners in the setup are strongly polarization dependent it is necessary to control the polarization of the circulating field in order to keep ring losses as low as possible. However, the polarization state of the circulating light varied with wavelength, and could only, to some extent, be compensated by the polarization controllers. However, it in spite of iterative re-optimization both polarization controllers, it was only possible to achieve sufficient control within a certain wavelength window. The center wavelength of the emission window could be shifted by up to ~5 nm using the polarization controllers, while the emission bandwidth remained almost constant.

### SWEPT FILTER SUPERFLUORESCENT YDFA SOURCE

Direct filtering of the output from a superfluorescent source, is a swept source configuration that offers low output power. However, it does not suffer from the power penalty related to an increased the scanning speed, as in the case of the scanning laser source. Furthermore, the full superfluorescent spectrum from the source is available for tomography.

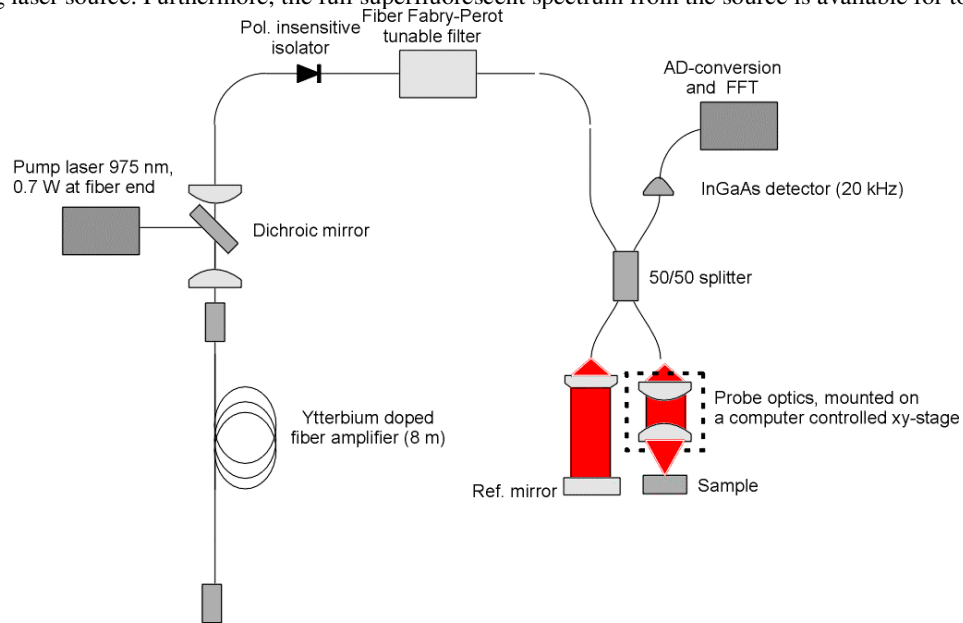


**Figure 4: Swept filter superfluorescent source and imaging setup.**

With the amplifier and tunable filter used in the laser experiments, a source based on filtering the reverse propagating superfluorescent output from an YDFA was therefore constructed. The output was coupled to a Michelson interferometer and used for tomographic imaging. The source and imaging setup is shown in Figure 4.

The scanned wavelength range was 25 nm, and the resolution was experimentally determined to be  $<40 \mu\text{m}$ . The output power of the superfluorescent source was 4 mW. Filtering and insertion losses limited the available power at the interferometer to  $\sim 10 \mu\text{W}$ . Yet, in spite of this limitation it is still possible to perform tomographic imaging of non-scattering samples, as illustrated in Figure 6, where the surface tomography of a coin is shown. Scanning speed was in these measurements limited by the detector, which had a bandwidth of 20 kHz.

The interferogram showed in Figure 5 (a) was obtained with a mirror in the sample arm, and the corresponding depth information was gained from a fast Fourier transform of the interferogram is shown in Figure 5 (b).

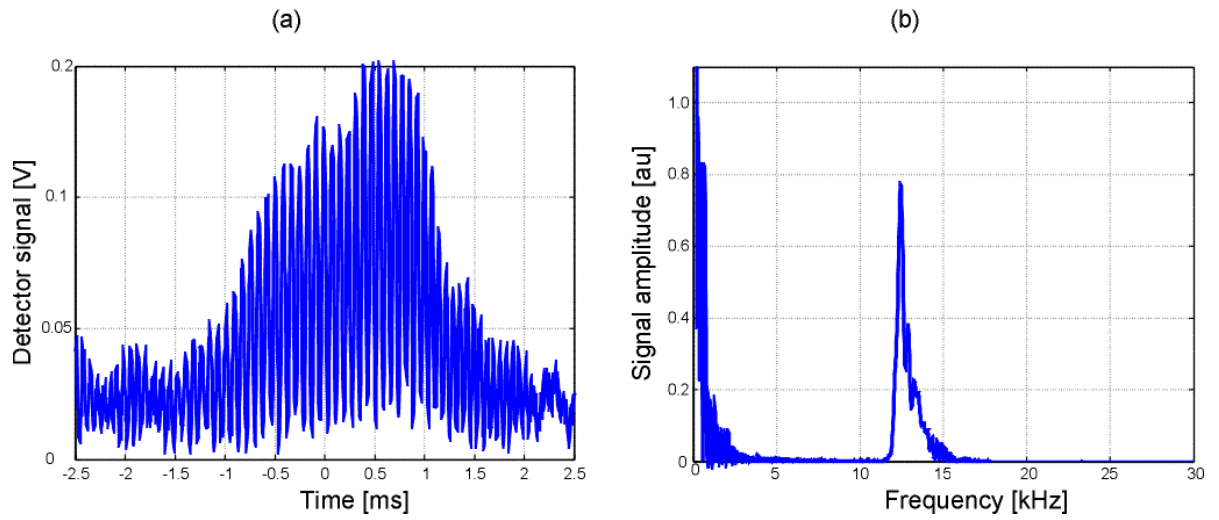


**Figure 5: Interferogram recorded with the swept filter superfluorescent setup (a) and frequency domain representation containing depth information**

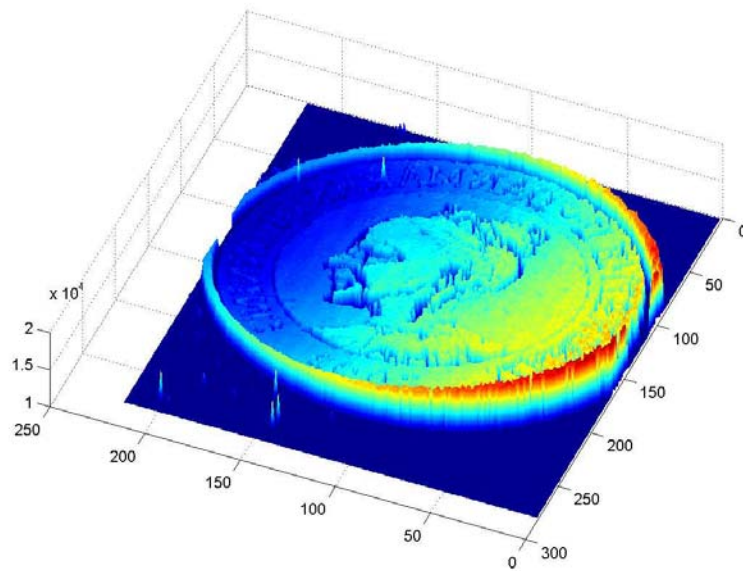


**Figure 6: Tomography of a coin recorded with swept filter superfluorescent setup**

## DISCUSSION

A linear power penalty in the output power from the scanning laser configuration was observed as the scanning frequency was increased. This power penalty is phenomena logically explained in Figure 7, where the normalized ring transmission, is shown along with the normalized spectrum of signal returning to the filter after a roundtrip in the cavity. Since the center wavelength of the filter has been shifted during the roundtrip time, only the hatched part of the spectrum will be transmitted, while in the remaining part of the transmission spectrum, lasing must be initiated from spontaneous emission. The upper state lifetime of the Yb<sup>3+</sup> in the amplifier is relative long, 0.8-1 ms [8]. Laser initiation from spontaneous emission is therefore slow, and is therefore a fundamental limitation in terms of scanning speed. Cavity length and filter bandwidth are factors available for optimization, cavity length should be kept short and filter bandwidth relative broad in order to reduce the power penalty.

In the present setup rather long passive fibers were used between isolators, filter and output coupler, resulting in a total ring length of 20 m.

It would be possible, to reduce the length of the passive fibers such that the total length of the cavity is limited primarily by the length of the amplifier (8 meters). Hence, it is expected that scanning speeds in the kHz range with sufficient output powers is feasible.

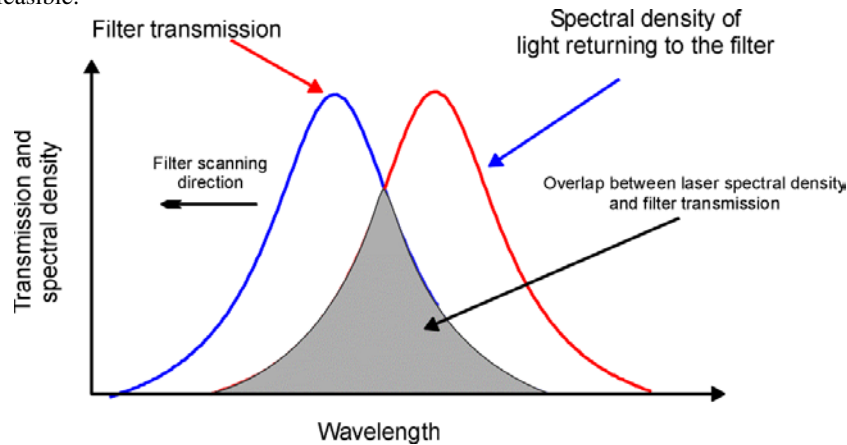


**Figure 7: The roundtrip delay in the cavity causes the filter transmission spectrum to shift relative to the laser spectrum returning to the filter**

The scanned wavelength range of the swept laser investigated was limited to 4 nm, and can be attributed to the combined effect of a relative high roundtrip loss and limited control of the polarization state. Experiments and theoretical investigations of a tunable ring laser based on Erbium doped amplifiers has shown the tuning range to be dependent on the saturation state of the amplifier [9]. The wavelength dependence of the gain in an EDFA decreases as saturation becomes stronger. In order to drive the amplifier in a more strongly saturated state, feedback to the amplifier should be strong, and hence roundtrip losses as low as possible. YDFAs are expected to exhibit a similar behavior. The insertion loss for the fiber-based isolators was 2 dB each, and wavelength dependent. Using free space, broad band isolators in the free space path between the amplifiers ends and the rest of the ring would decrease the ring loss by ~3 dB, and further improvements can be gained in reducing the output coupling ratio.

However, the present experiments showed that it was possible to change the center emission wavelength up to 4 nm by adjusting the polarization controllers. This indicates that the bandwidth was primarily limited by the wavelength dependent polarization state. Hence, improved polarization control has priority in the further development of the source.

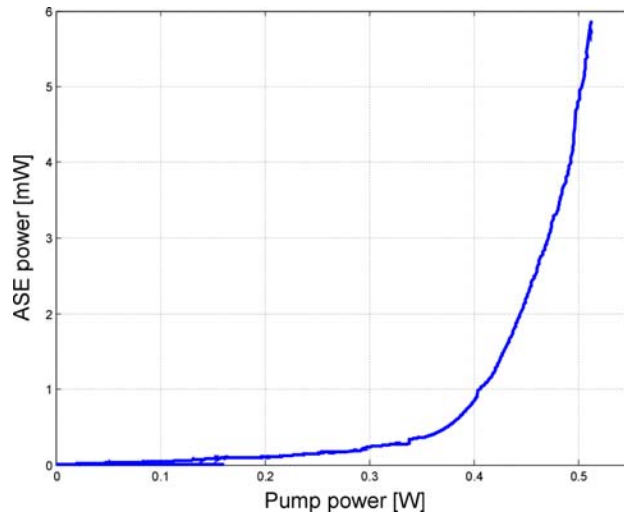


**Figure 8: Reverse propagating ASE power as a function of pump power**

The primary limitation for the filtered ASE source is the available power, limiting its applicability to non-scattering samples. The output power can be increased by increasing the pump power, as shown in Figure 8, where the total fluorescent power from the amplifier is shown as a function of pump power. However, this strategy also reduces the available bandwidth of the fluorescent spectrum as shown in Figure 9 where the fluorescent spectrum is shown for two pumping powers. Yet, with more complex designs of the fluorescent source output powers up to 30 mW has been demonstrated while retaining a bandwidth of 75 nm [10]. Subsequent amplification of the filtered output would make such source applicable for imaging of scattering samples, without the speed or bandwidth limitations associated with scanning laser configurations.

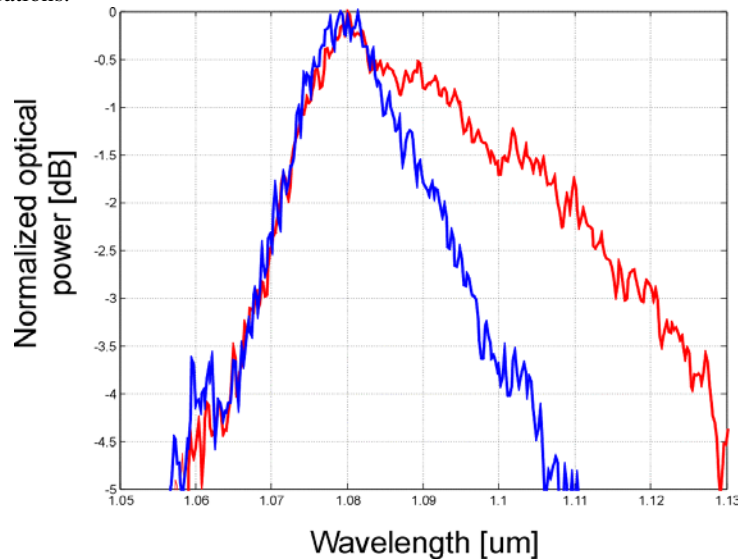


**Figure 9: ASE spectrum for high (blue) and low (red) pump power**

### CONCLUSION

Tomographic imaging with a tunable light source operating in the 1 um range has been demonstrated. By using a tunable filter in conjunction with an YDFA based superfluorescent light source it was possible to achieve an axial

resolution of  $<40 \mu\text{m}$ . The scanning speed was in the present case limited by the available detection system. With further development of the fluorescent source configuration, can improve the resolution to the sub-10  $\mu\text{m}$  range. With a ring laser based on a Ytterbium doped fiber amplifier it was possible to obtain a scanned bandwidth of 4 nm, experiments showed that improved polarization control can increase the bandwidth by 50% and scanning speeds up to the kHz range is possible.

### ACKNOWLEDGEMENT

The authors would like to thank the Danish Research Agency for financial support under the framework program BIOLASE, grant number 26-02-0020, and Micron Optics for supplying a tunable filter and technical support.

- 
1. M. A. Choma, M. V. Sarunic, C. Yang and J. A. Izatt, "Sensitivity Advantage of Swept Source and Fourier Domain Optical Coherence Tomography", *Opt. Express* **11**, 2183-2189 (2003)
  2. U. Haberland, W. Rütten and V. Blazek and H. J. Schmitt, "Investigation of Highly Scattering Media Using Near-Infrared Continuous Wave Tunable Semiconductor Laser", in *Optical Tomography, Photon Migration, and Spectroscopy of Tissue and Model Media: Theory, Human Studies, and Instrumentation*, Britton Chance and Robert R. Alfano, eds., Proc. SPIE 2389, 503-512 (1995)
  3. B. Povazay, K. Bizheva, B. Hermann, A. Unterhuber, H. Sattmann, A.F. Fercher, C. Schubert, P.K. Ahnelt, M. Mei, R. Holzwarth, W. J. Wadsworth, J.C. Knight and P. St. J. Russel, "Enhanced Visualization of Choroidal Vessels Using Ultrahigh Resolution Ophthalmic {OCT} at 1050 nm", *Opt. Express* **11**, 1980-1986 (2003)
  4. A. Unterhuber, B. Povazay, B. Hermann, H. Sattmann, A. Chavez-Pirson and W. Drexler, "In vivo retinal optical coherence tomography at 1040 nm - enhanced penetration into the choroid", *Opt. Express* **13**, 3252-3258 (2005)
  5. S.H. Yun, C. Boudoux, M.C. Pierce, J.F. de Boer, G.J. Tearney and B.E. Bouma, "Extended-Cavity Semiconductor Wavelength-Swept Laser for Biomedical Imaging" *IEEE Photon. Technol. Lett.* **16**, 293-295 (2004)
  6. A. Hideur, T. Chartier, C. Özkul and F. Sanchez, "Dynamics and Stabilization of a High Power Side-Pumped Yb-Doped Double-Clad Fiber Laser", *Optics Comm.* **186**, 311-317 (2000)
  7. M. Auerbach, P. Adel, D. Wandt, C. Fallnich, S. Unger, S. Jetschke and H.-R. Müller, "10 W Widely Tunable Narrow Linewidth Double-Clad Fiber Ring Laser", *Opt. Express* **10**, 139-144 (2002)
  8. H.M. Pask, R.J. Carman, D.C. Hanna, A.C. Tropper, C.J. Mackechnie, P.R. Barber and J.M. Dawes, "Ytterbium-Doped Silica Fiber Lasers: Versatile Sources for the 1-1.2  $\mu\text{m}$  Region", *IEEE J. Select. Topics Quantum Electron* **1**, 2-13 (1995)
  9. A. Bellemare, M. Karásek, C. Riviere, F. Babin, G. He, V. Roy and G. W. Schinn, "A Broadly Tunable Erbium-Doped Fiber Ring Laser: Experimentation and Modeling", *IEEE J. Select. Topics Quantum Electron.* **7**, 22-29 (2001)
  10. S.V. Chernikov, J.R. Taylor, V.P. Gapontsev, B.E. Bourma and J.G. Fujimoto, "A 75nm, 30 mW superfluorescent ytterbium fiber source operating around 1.06  $\mu\text{m}$ " *CLEO* (1997)